Astronomical and Astrophysical Transactions (*AApTr*), 2016, Vol. 29, Issue 3, pp. 277–282,
ISSN 1055-6796, Photocopying permitted by license only, ©Cambridge Scientific Publishers

Upper limits on the extragalactic magnetic fields from the NVSS rotation measures

M.S. Pshirkov[1,2,3,*], P.G. Tinyakov[4], F.R. Urban[4]

[1] *Sternberg Astronomical Institute, Lomonosov Moscow State University, Universitetsky Prospekt 13, 119992, Moscow, Russia*
[2] *Institute for Nuclear Research, Russian Academy of Sciences, 117312, Moscow, Russia*
[3] *Pushchino Radio Astronomy Observatory, 142290 Pushchino, Russia*
[4] *Université Libre de Bruxelles, Service de Physique Théorique, CP225, 1050, Brussels, Belgium*

Received 15 September, 2015

The rotation measures data from the NVSS catalogue are used to construct upper limits on the strength of extragalactic magnetic fields. If present, these fields would give rise to a contribution to the rotation measures which grows with the distance. As observations show that low-luminosity distant radio sources do not exhibit any trend with their redshift, extragalactic fields with Mpc coherence length could be constrained to be below approximately 1.5 nG; a field with a present horizon size coherence length is bounded to be below 0.6 nG. These limits do not depend on the particular origin of these cosmological fields.

Keywords: Extragalactic magnetic fields, ultra-high energy cosmic rays, Faraday rotation measures

1 Introduction

MFs are ubiquitous in the Universe, from planets to clusters of galaxies (Vallée (2004); Kronberg (1994); Durrer & Neronov (2013)); but still on the largest spatial scales cosmological magnetic fields remain elusive. One of the signatures of these MFs would be the rotation of polarisation planes of electromagnetic waves propagating from distant sources to the Earth. In Pshirkov et al. (2014) it was shown that Faraday rotation measures (RMs) of far-away less luminous radio sources do not demonstrate any significant evolution with redshift. Presence of extragalactic MF (egMF) of certain strength could lead to an evolution of RM distribution with distance. Thus this non-observation of any evolution could be used to constrain egMFs by a comparison of simulated and observed RMs distributions.

*Email: pshirkov@sai.msu.ru

The strongest current upper limits on the strength, $\hat{B}$, of present-day egMFs come from microwave background observations by the Planck Collaboration (2015): $\hat{B} \lesssim 3$ nG for a coherence length $l_c = 1$ Mpc. It should be noted, that these limits apply only to primordial MFs, i.e., fields generated in the very early Universe, however, cosmological MFs could be generated at later stages by various astrophysical mechanisms (e.g. Kronberg et al. (2001)).

Previous analyses of RM data produced weaker limits: the same $l_c = 1$ Mpc field is bound to have $\hat{B} \lesssim 6$ nG (Blasi et al. (1999)). With our method, and new available RM data, these limits were improved fourfold or more: egMFs with coherence lengths of 1 Mpc and strengths above 1 nG are highly incompatible with current RM observations; this limit becomes about twice as strong if the egMF have a horizon size coherence length.

2 Method

2.1 Data

The plane of polarisation of a linearly polarised electromagnetic wave, which moves through a magnetised plasma, rotates by an angle φ proportional to the square of the wavelength λ: $\varphi = \mathrm{RM}\,\lambda^2$, where

$$\mathrm{RM} = 812 \int_D^0 n_\mathrm{e} B_{||}\,\mathrm{d}l, \tag{1}$$

where n_e is the density of free electrons measured in cm^{-3}, $B_{||}$ is the component of the MF parallel to the line of sight (in μG), and D is the distance to the source in kpc; RM is measured in $\mathrm{rad/m}^2$.

The largest set (to date) of RM of extragalactic sources was compiled in Taylor et al. (2009), using the NRAO VLA Sky Survey (NVSS) data (Condon et al. (1998)). This set comprises 37,543 sources, 4002 out of them have known redshifts (Hammond et al. (2012)). From the latter sub-set, the sources with galactic latitude $|b| > 20°$, $|\mathrm{RM}| < 300$ rad m^{-2} were accepted.

The observed RM could be split as $\mathrm{RM_{obs}} = \mathrm{RM_{gal}} + \mathrm{RRM}$, where the first term is the contribution of the regular MF of the Milky Way, and the second term stands for "residual RM", and includes all other contributions to RM other than the local (regular) MF: RM instrinsic to the source, measurement errors, turbulent galactic MF, and egMF (RRMx).

First of all, redshift-dependent effects should be isolated from those intrinsic to sources themselves, thus their luminosity at 1.4 GHz was computed using the spectral indices from Farnes et al. (2014). As not all sources have measured spectral indices that reduced the total number of objects in the set to 3051. After that, the set was split into two groups using a luminosity threshold of $L_{1.4\mathrm{GHz}} = 10^{27.8}$ W Hz^{-1}: the low luminosity group consists of 2593 sources, while the high luminosity one includes 458 of them. After subtraction of the $\mathrm{RM_{gal}}$ contribution from $\mathrm{RM_{obs}}$, giving RRMs. For the lower power group, RRMs do not evolve with redshift and, subsequently, this is the data employed in this work. Table 1 demonstrates this observation.

Table 1 Upper bin redshift boundaries z_b, numbers of sources in the bin N_s, and their averages $\langle|\mathrm{RRM}|\rangle$, for the low-power group.

z_b	0.15	0.35	0.7	1.3	1.65	1.95	2.25	2.6	5
N_s	418	418	501	677	291	137	76	50	25
$\langle\|\mathrm{RRM}\|\rangle$	16.2	15.3	15.9	16.6	15.4	15.8	16.2	13.9	16.3

2.2 Simulations

The extragalactic MFs, if present, affect observed RMs (Blasi et al. (1999); Akahori & Ryu (2011)). The RRMx would grow with redshift. So, the observed redshift independent behaviour could not be compatible with presence of sufficiently strong magnetic field. Thus, by simulating the effects of this hypothesised egMF its strength could be constrained.

An essential part of simulation is the model of electron density distribution. It is assumed to follow the observed Lyman-α (Lyα) forest distribution of neutral hydrogen absorption lines (Blasi et al. (1999); Akahori & Ryu (2011)). A simple analytical approximation from (Bi & Davidsen, 1997; Coles & Jones, 1991) was employed, which is a standard log-normal distribution for the electron overdensity, δ_e, with scale parameter

$$\sigma_\mathrm{e}(z) = 0.08 + \frac{5.37}{(1+z)} - \frac{4.21}{(1+z)^2} + \frac{1.44}{(1+z)^3}\,,$$

and location $\mu_\mathrm{e}(z) = -\sigma_\mathrm{e}^2(z)/2$:

$$P(\delta_\mathrm{e}) = \frac{1}{\sqrt{2\pi}\sigma_\mathrm{e}(1+\delta_\mathrm{e})} \exp\left\{-\frac{[\ln(1+\delta_\mathrm{e}) - \mu_\mathrm{e}(z)]^2}{2\sigma_\mathrm{e}^2}\right\}. \qquad (2)$$

This distribution is accurate for fluctuations at the Jeans length scale $\lambda_J(z) \simeq 2.3(1+z)^{-3/2}$ Mpc (Bi & Davidsen (1997)) ($H_0 = 71$ km/s/ Mpc as the Hubble parameter today and $\Omega_M = 0.27$ as the total matter density fraction are adopted). The actual electron density is finally expressed as $n_\mathrm{e}(z) = n_\mathrm{e}(0)(1+\delta_\mathrm{e})(1+z)^3$, with $n_\mathrm{e}(0) = 1.8 \times 10^{-8}$ cm^{-3}.

The MF model is rather simple and is characterised by only two parameters: its strength $\hat{B}$ and its coherence length l_c. Two values for l_c were tested: the Jeans length λ_J and the Hubble size $1/H_0$. The MF is frozen into the plasma; thus, for spherical overdensities, it will evolve accordingly as $B(z) = \hat{B}\,[n_\mathrm{e}(z)/n_\mathrm{e}(0)]^{2/3}$.

A large number of lines of sight in steps of λ_J up to some given redshift were generated. The electron density is generated at each step sampling the distribution (2), the randomly oriented MF was simulated, with recalculation of its amplitude each time the distance travelled equals a multiple of the correlation length.

The expected theoretical egMF-induced |RRMx| evolution curves with redshift were obtained, by averaging 10^5 lines of sight out to redshift $z = 5$: the result is given in Fig. 1 for a benchmark MF reference value of $\hat{B} = 1$ nG: the rapid increase of |RRMx| with redshift is clearly seen. There is a sharp transition in the behaviour of RRMx(z) roughly localised between $z = 0.5$ and $z = 1$: for $l_c = 1/H_0$ the growth of RM is significantly suppressed at high redshifts, whereas if $l_c = \lambda_J$ the curve becomes essentially flat.

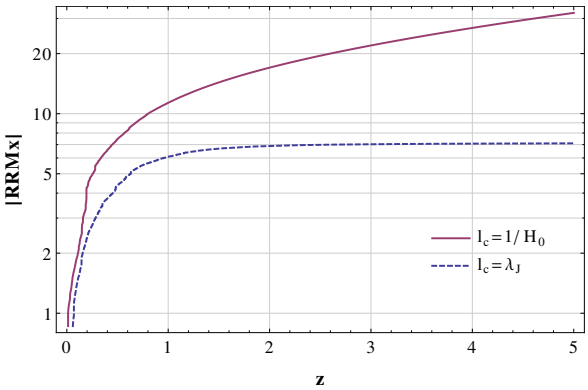


Figure 1 Theoretical |RRMx| evolution with redshift for $l_c = \lambda_J$ (blue, dashed), and $l_c = 1/H_0$ (red, solid), averaged for 10^5 lines of sight.

These theoretical simulations could account for only the contribution from the egMF: the contributions from the turbulent Galactic fields, measurement errors, and intrinsic RMs could not be simulated in this way. Contributions due to the turbulent field and instrumental errors are dominant and redshift-independent; intrinsic contribution depends on redshift but it is subdominant. The information about these redshift-independent contributions could be extracted from low-z data, after that the high-redshift portion of the data could be compared with the simulated distributions for the same set of sources, with the addition of egMF.

Everything is split in three redshift bands: we take the low redshift set to correspond to bins 1 and 2 of Table 1, that is, $z = [0, 0.35]$, the high redshift set from $z \geq 1.3$ (that is, bins 5 to 9), and a transition set, which was left unused, corresponding to bins 3 and 4, or $z = [0.35, 1.3]$. The three sets contain 836, 1178, and 579 sources, respectively.

The *simulated* distribution of |RRM| at high-z was constructed as follows (see Pshirkov et al. (2015) for details). First one RRM was randomly picked from the low-z set: this is an estimation of the z-independent contribution which cannot be simulate in our model. Then, a second batch of RRMx values is generated by simulating 100 lines of sight for each of the sources of the high-z set, that is, a total of 57900 lines of sight. This RRMx is generated for our benchmark field value of $\hat{B} = 1$ nG, and then rescaled for any other value of $\hat{B}$, simulating the egMF contribution we are seeking. Randomly picked values from both batches (one each) are then incoherently added (that is, each with its own sign) 10^5 times to generate the final theoretical |RRM| distribution, as a function of the MF strength and coherence length. This distribution in the end is compared with the actual data.

3 Results

Two distributions – the data, and the theoretical predicted sample – are compared by means of a Kolmogorov–Smirnov (KS) test. This test allows us to use all of the information contained in the distributions, not only first moments in a given redshift

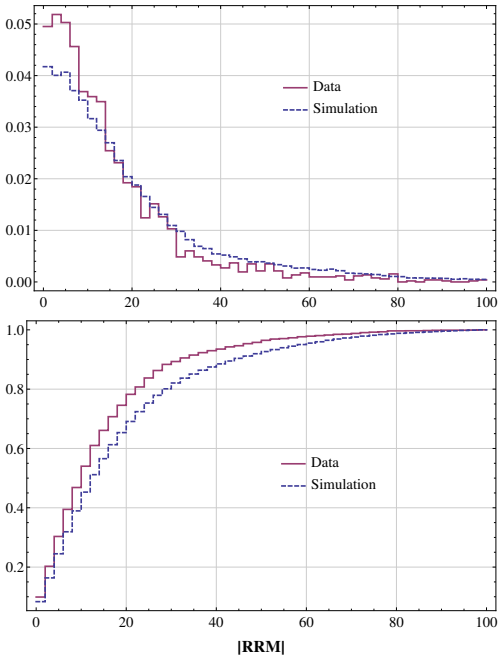


Figure 2 PDF and CDF showing |RRM| for the data (blue, dashed) and a simulated |RRM| with $\hat{B} = 3$ nG and $l_c = \lambda_J$ (red, solid).

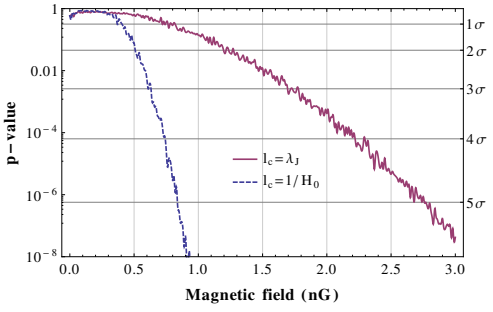


Figure 3 p-Values as a function of $\hat{B}$ for $l_c = \lambda_J$ (blue, dashed), and $l_c = 1/H_0$ (red, solid) obtained from KS test.

bin. Example of this comparison is shown in Fig. 2, for $\hat{B} = 3$ nG and $l_c = \lambda_J$, the two distributions are statistically incompatible. In this figure an example of the PDFs and CDFs of the two distributions that are compared is presented: the data and a simulated |RRM| with $\hat{B} = 3$ nG and $l_c = \lambda_J$. It is clear that such a field value is strongly disfavoured – the two distributions are statistically incompatible.

Figure 3 shows the p-values of the KS tests as a function of $\hat{B}$ for both the $l_c = \lambda_J$ (blue, dashed), and $l_c = 1/H_0$ (red, solid) cases. For an egMF with $l_c = \lambda_J$ the values

of $\hat{B}$ corresponding to p-values of 1σ, 2σ, and 3σ are $\hat{B} = 0.65$ nG, $\hat{B} = 1.2$ nG, and $\hat{B} = 1.7$ nG, respectively. For the Hubble-scale case the limits are stronger: 3σ level is already reached at $\hat{B} = 0.6$ nG.

4 Conclusion

Extragalactic MF with coherence lengths of 1 Mpc cannot be stronger than 1.7 nG (at the 3σ level), whereas a Hubble-scale egMF is bound to be weaker than about 0.6 nG. These limits are obtained using RM data from extragalactic sources, and are valid independently of the origin of these egMF given that they are present at $z < 3$. They are at least a four times improvement over those previously available in the literature that were obtained with RM, and are now competitive with microwave background ones, which however apply only to primordial fields, e.g. existing already at $z \sim 1000$.

These limits are important to ultra high-energy cosmic ray (UHECR) propagation: if an egMF with $\hat{B} \simeq 1$ nG and $l_c \simeq \lambda_J$ existed, they would deflect UHECRs significantly. The median deflection for a proton primary of even the highest energy, 10^{20} eV, would be around 9 deg when propagating from a distance of 200 Mpc. This comes as a result of a simulation with particular (Lyα) B distribution rather than simplified cell models usually implemented in previous estimates.

Acknowledgements

The work was supported by a grant of the President of the Russian Federation (MK-4167.2015.2) and an RFBR grant (14-02-00657). The author acknowledges the fellowship of the Dynasty foundation.

References

Akahori T., Ryu D., (2011), Astrophys. J., 738, 134
Bi H., Davidsen A. F., (1997), Astrophys. J., 479, 523
Blasi P., Burles S., Olinto A. V., (1999), Astrophys. J., 514, L79
Coles P., Jones B., (1991), Mon. Not. Roy. Astron. Soc., 248, 1
Condon J. J., Cotton W., Greisen E. et al., (1998), Astron.J., 115, 1693
Durrer R., Neronov A., (2013), Astron. Astrophys. Rev., 21, 62
Farnes J., Gaensler B., Carretti E., (2014), Astrophys. J. Suppl., 212, 15
Hammond A. M., Robishaw T., Gaensler B. M., (2012), arXiv:1209.1438 [astro-ph.CO]
Kronberg P. P., (1994), Rept. Prog. Phys., 57, 325
Kronberg P. P., Dufton Q. W., Li H. et al., (2001), ApJ, 560, 178
Planck Collaboration, (2015), arXiv:1502.01594
Pshirkov M., Tinyakov P., Urban F., (2015), Mon. Not. Roy. Astron. Soc., 452, 2851
Pshirkov M. S., Tinyakov P. G., Urban F. R., (2015), arXiv:1504.06546
Taylor A., Stil J., Sunstrum C., (2009), Astrophys. J., 702, 1230
Vallée J. P., (2004), New Astron. Rev., 48, 763